Article

Assessment of the structural efficiency of materials of a monitoring agrorobot frame based on differential micro-spraying technology

Sardor Suyunov [1]*, Sherzod Barlibayev [1], Abdurahmon Rasuljonov [2], Islom Tangirov [2]

[1] Department of Metrology and Engineering Tashkent Institute of Irrigation and Agricultural Mechanization Engineers National Research University
Tashkent, 100000, Uzbekistan : sardor.suyunov.93@gmail.com (S.S.), barlibayev.phd@gmail.com (Sh.B.)
[2] Scientific Research Institute of Agricultural Mechanization
Tashkent, 100000, Uzbekistan abduraxmon.rasuljonov@gmail.com (A.R.), tangirovislom7@gmail.com (I.T)

* Correspondence: sardor.suyunov.93@gmail.com; Tel.: +998 93 5768557 (S.S.)

Abstract: Nowadays, the protection of agricultural crops from various diseases and pests is traditionally carried out through the application of chemical spraying agents. However, this spraying method has negative environmental impacts, causing soil and water contamination. This article presents the results of a study aimed at evaluating the structural performance and strength characteristics of agrorobot frame materials, developed for crop protection against diseases and pests as well as field condition monitoring, using ANSYS software.

Keyword: Agricultural robot frame; static structural analysis; structural steel; aluminum alloy; total deformation; equivalent stress; elastic deformation; thermal deformation; ANSYS simulation; CAD/CAE modeling; mechanical strength; thermal stability.

Quoting: Sardor Suyunov, Sherzod Barlibayev, Abdurahmon Rasuljonov, Islom Tangirov. Agroengineering Solutions. **2026**, 3, 4, 1 https://doi.org/10.35938/AY-2026-3-00001

Received: 06.05.2026
Corrected: 02.06.2026
Accepted: 04.07.2026
Published: 08.07.2026

Introduction

With the growth of the global population, the demand for food is increasing rapidly. Meeting this growing demand is considered one of the major challenges facing modern agriculture. According to recent studies, global food demand is expected to rise significantly by 2050 [1]. The scale of this increase is directly influenced by population growth, income levels, and climate change. Research conducted by M.V. van Dijk, T. Morley, M.L. Rau, and Y. Saghai [2] predicts that between 2010 and 2050, total global food demand will increase by 35% to 56%, while when climate change is considered, this range may vary from 30% to 62%. Furthermore, studies by W.P. Falcon, R.L. Naylor, and N.D. Shankar [3] estimate that global food demand will rise by 50% to 60% from 2019 to 2050.

Meeting the growing food demands of the population can be achieved not only through traditional agricultural mechanization methods, but also through the implementation of smart agricultural technologies integrated with artificial intelligence [4].

Considering the aforementioned challenges, an agrorobot design based on differential micro-spraying technology was developed. This system enables early detection of crop diseases, monitoring of soil conditions and water availability, yield forecasting, and effective control of plant diseases and pests (Figure 1).

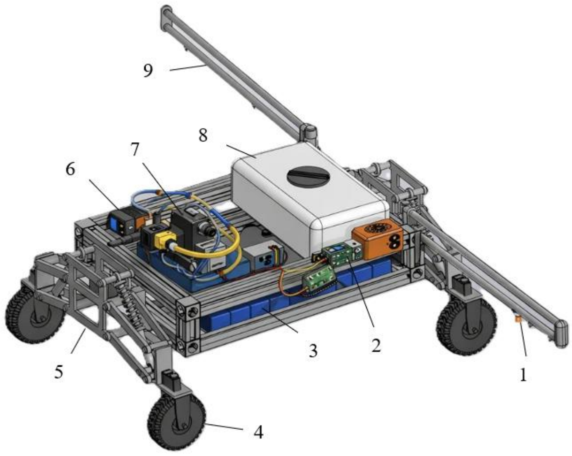

1 – Nozzle; 2 – Microcontroller; 3 – Batteries; 4 – Brushless motorized wheels; 5 – Shock absorption mechanism; 6 – Sensors and hyperspectral camera; 7 – Pump and filtration system; 8 – Chemical solution tank; 9 – Spray boom.

Figure 1. Structural design of the agrorobot platform based on differential micro-spraying technology.

The field performance of the proposed agricultural robot, including its mobility, maneuverability, load-carrying capacity, and resistance to becoming stuck under challenging terrain conditions, largely depends on the material selected for its frame and chassis structure. In practice, robot chassis systems are commonly manufactured from materials such as aluminum alloys or structural steel, similar to vehicle body structures. Therefore, ensuring high strength, reliability, and durability in chassis design is of critical importance. In engineering applications, optimizing the weight and dimensions of the robot chassis and body remains one of the primary challenges [5].

The use of lightweight materials in the robot's structural components contributes to reduced overall mass, optimized energy consumption, improved mobility efficiency, and enhanced operational stability. However, due to the complexity of agricultural environments, including uneven terrain, external mechanical loads, and dynamic stresses encountered during operation, the chassis and frame components must also possess sufficient mechanical strength, deformation resistance, and long-term durability [6,7].

In mechanical engineering, steel is widely used for manufacturing structural and housing components due to its high strength, durability, weldability, and relatively low cost. However, compared to alternative materials, steel has a significantly higher density, which increases overall structural weight. Aluminum alloys, on the other hand, offer lower weight and superior corrosion resistance, although their mechanical strength is generally lower and their cost is typically higher than that of steel [8].

While steel provides excellent structural integrity, its greater mass can reduce the energy efficiency of agricultural robots. Conversely, aluminum alloys enable the development of lightweight structures, but they may exhibit higher deformation under operational loads. Therefore, selecting the optimal frame material for agricultural robots represents an important scientific and engineering challenge in balancing structural safety, durability, and energy efficiency [9].

Although reducing the structural mass of an agrorobot improves energy efficiency, maintaining sufficient structural strength remains a significant engineering challenge [10]. Numerous scientific studies have been conducted on the appropriate selection of materials and the optimization of agrorobot structural designs.

In research carried out by Avadhoot Rajurkar, Kunal Dangra, Aryan Deshpande, Madhav Gosavi, Tejas Phadtare, and Gajanan Gambhire, aluminum alloy and structural steel were comparatively evaluated for a three-wheeled robot chassis intended for operation under uneven field conditions using SolidWorks simulation analysis. The results demonstrated that structural steel exhibited superior strength and deformation resistance, whereas aluminum alloy, despite its lower weight, showed greater susceptibility to deformation. The study emphasized the importance of comprehensively considering load, acceleration, and thermal factors when selecting materials for robot chassis design [11].

An innovative robot for harvesting lettuce leaves was developed by Ruoyuan Liu, Mingjie Dong, Qi Xiao, Changqi Lv, and Ziqiang Zhang. To reduce energy consumption, improve maneuverability, and minimize soil pressure, the robot frame was designed to be lightweight. For this purpose, aluminum profiles were selected as the primary structural material. Based on the assembled frame, structural simulation analysis was performed using SolidWorks, which demonstrated that the deformation and stress values at the three critical connection points were significantly below allowable limits [12].

Studies conducted by Renkai Ding, Xiangyuan Qi, Xiangpeng Meng, Xuwen Chen, Le Zhang, Yixin Mei, Anze Li, and Qing Ye examined the mobility, stability, and field adaptability of wheeled, tracked, and hybrid chassis agricultural robots. Their findings identified the advantages and limitations of each chassis configuration and outlined future directions for the development of more intelligent and adaptable agricultural robotic platforms [13].

Although previous research has extensively investigated the functional capabilities of agricultural robots, insufficient attention has been given to comparative analyses of structural performance and energy efficiency for identical designs manufactured from different materials under realistic field conditions. ANSYS Workbench simulation enables preliminary evaluation of agrorobot structural resistance under operational loading conditions. Therefore, the purpose of this study is to compare steel- and aluminum alloy-based agrorobot frame designs in terms of structural strength, deformation behavior, and safety performance using ANSYS Workbench.

2 Materials and Methods

In this study, the developed four-wheeled agrorobot frame was analyzed from a static structural perspective, focusing on key mechanical performance indicators such as total deformation, equivalent stress, equivalent strain, thermal deformation, and related structural parameters. Aluminum alloy and structural steel were selected as frame materials, and their structural performance was comparatively evaluated.

The three-dimensional structural model of the agrorobot was developed in the COMPAS-3D CAD environment. The completed model was then exported to ANSYS Workbench in STEP format for further structural simulation and analysis.

During the ANSYS simulation process, standard engineering modeling and analysis procedures were applied. Initially, according to the design specifications and technical requirements, the robot frame was designed as a CAD model in COMPAS-3D.

Subsequently, the prepared model was imported into the ANSYS Workbench environment, where the necessary simulation parameters were configured. Based on load-bearing capacity, weight optimization criteria, and materials database properties, two candidate materials—aluminum alloy and structural steel—were selected for comparative analysis.This section may be divided by subheadings. It should provide a concise and precise description of the experimental results, their interpretation as well as the experimental conclusions that can be drawn.

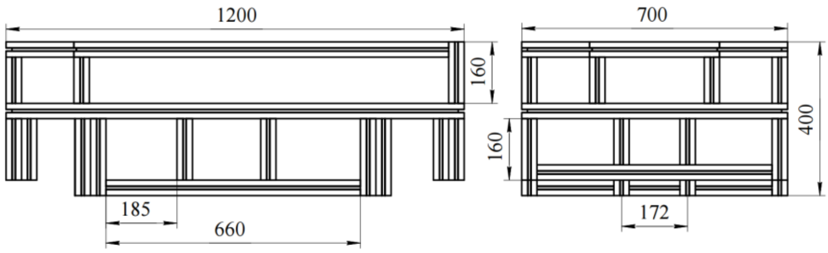

a)

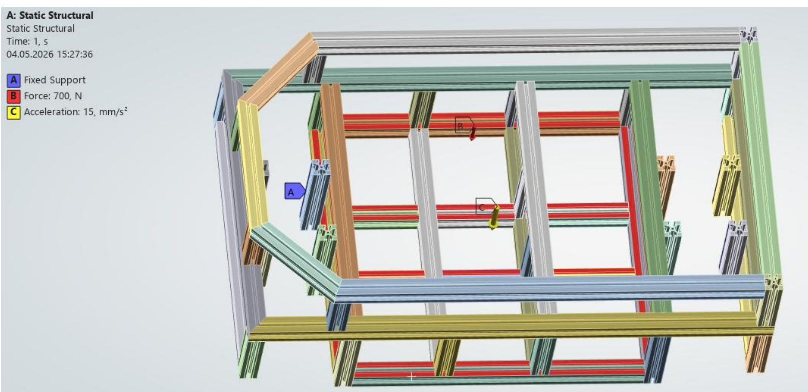

b)

Figure 2. (a) Robot frame drawing, (b) application of forces, acceleration and fixed support forces on the frame, acceleration and fixed support on the frame

The 2D drawing of the robot frame and its three-dimensional model are shown in Figures 2 (a)–(b), respectively. The main properties of the materials used in the simulation are described in detail in Tables 1 and 2.

Table 1. Aluminum Alloy Specification used in Ansys

Property	Value	Property	Value
Young's Modulus	71000 MPa	Compressive Ultimate Strength	0 MPa
Poisson's Ratio	0,33	Compressive Yield Strength	280 MPa
Bulk Modulus	69608 MPa	Tensile Ultimate Strength	310 MPa
Shear Modulus	26692 MPa	Tensile Yield Strength	280 MPa
Isotropic Secant Coefficient of Thermal Expansion	295,15 K		

Table 2. Structural Steel Specification used in Ansys

Property	Value	Property	Value
Young's Modulus	200000 MPa	Compressive Ultimate Strength	0 MPa
Poisson's Ratio	0,3	Compressive Yield Strength	250 MPa
Bulk Modulus	166700 MPa	Tensile Ultimate Strength	460 MPa
Shear Modulus	76923 MPa	Tensile Yield Strength	250 MPa
Isotropic Secant Coefficient of Thermal Expansion	273,15 K		

3 Results & Discussion

3.1 Frame behavior under static load conditions.

According to the results of the static structural analysis performed in the ANSYS environment, when only external loading was applied to the robot frame, the maximum total deformation was primarily concentrated in the central lower section of the frame. Minimal deformation was observed in the support regions and rigidly fixed structural components.

In the deformation distribution map, the red and yellow zones indicate regions subjected to the highest deformation, whereas the blue zones represent areas with relatively low deformation and greater structural stability. The increased deformation in the central structural elements suggests that load concentration is highest in this region. Meanwhile, the front, rear, and upper sections of the frame remained comparatively stable under the applied loading conditions.

Based on the obtained results, the robot frame demonstrates sufficient mechanical strength under operational loads considering the selected material properties and geometric configuration. However, the relatively higher deformation observed in the central load-bearing region is mainly attributed to the absence of direct support in this area.

Comparative analysis showed that the aluminum alloy frame experienced greater total deformation than the structural steel frame. This is primarily due to the lower tensile strength and stiffness characteristics of aluminum alloy compared to structural steel (Figures 2 and 5).

Although equivalent stress values were generally similar for both materials, slightly higher stress values were observed in structural steel (Figures 3 and 6). In contrast, equivalent elastic strain was more pronounced in the aluminum alloy frame, which is associated with its relatively greater susceptibility to deformation (Figures 4 and 7).

The total deformation, equivalent stress, and the maximum and average strain values for the aluminum alloy frame are presented in Table 3, while the corresponding results for the structural steel frame are provided in Table 4.

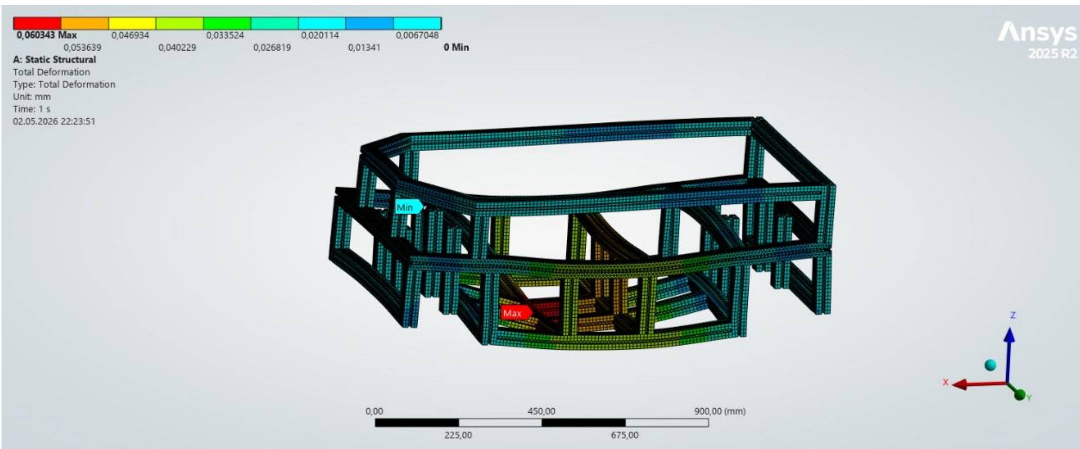

Fig. 3. Total deformation of the aluminum alloy frame without considering thermal and acceleration effects.

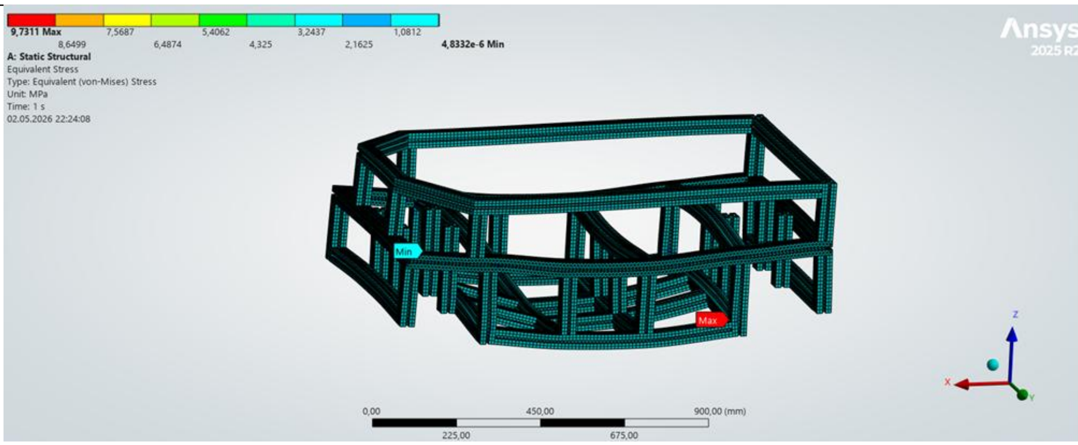

Fig. 4. Equivalent Stresses of the aluminum alloy frame without thermal and acceleration condition

Fig. 5. Equivalent Elastic Strain of aluminum alloy chassis without thermal and acceleration conditions

Table 3. Aluminum Alloy without thermal and acceleration condition

	Maximum Value	Average Value
Total Deformation (mm)	0,060343	0,017338
Equivalent Stress (MPa)	9,7311	0,26121
Equivalent Elastic Strain	0,00013706	0,0000041632

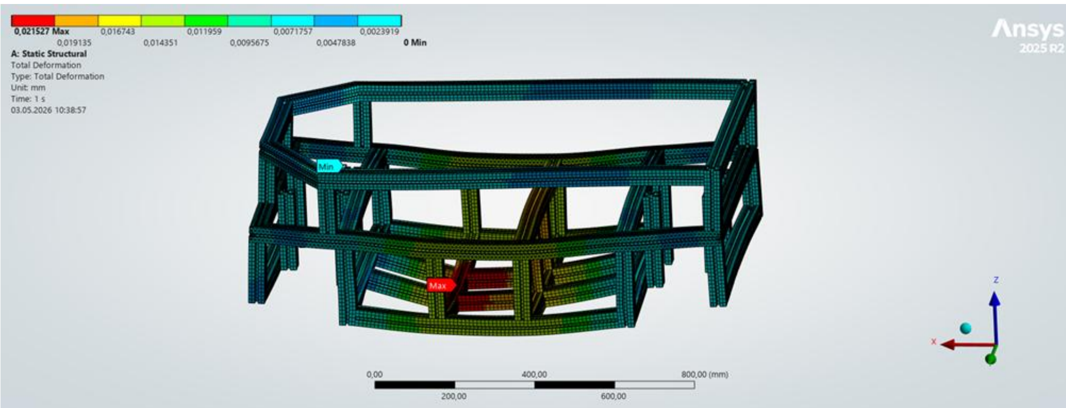

Fig. 6. Total deformation of structural steel frame without thermal and acceleration conditions

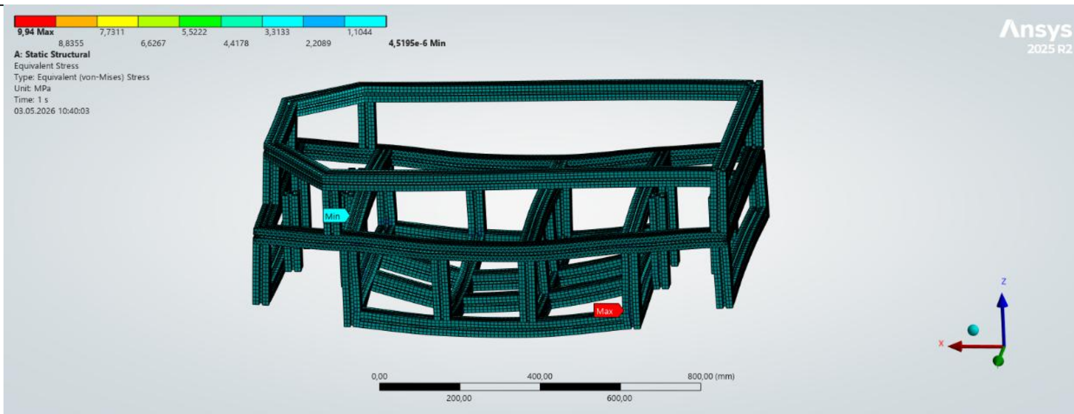

Fig. 7. Equivalent stresses of structural steel frame without thermal and acceleration conditions

Fig. 8. Equivalent elastic strain of structural steel frame without thermal and acceleration conditions

Table 4. Structural Steel without Thermal and Acceleration conditions

	Maximum Value	Average Value
Total Deformation (mm)	0,021527	0,0061718
Equivalent Stress (MPa)	9,94	0,26066
Equivalent Elastic Strain	0,0000497	0,0000014879

3.2 Frame condition under combined loading and acceleration effects.

According to the results of the conducted analyses, when the robot frame is subjected to external loading together with the acceleration effect, the structural steel configuration exhibits lower total deformation compared to the aluminum alloy design. This behavior is attributed to the higher strength and stiffness properties of steel (Figures 8 and 11).

In the comparative analysis, it was observed that the equivalent stress levels in the structural steel frame are slightly higher than those in the aluminum alloy structure. In the aluminum design, this parameter is relatively lower, which is associated with the material's more pronounced elastic response under loading conditions (Figures 9 and 12).

The analysis of elastic deformation results indicates that dimensional changes in the structural steel frame are smaller than those in the aluminum alloy frame, confirming the higher deformation resistance of steel (Figures 10 and 13).

It was also found that the inclusion of the acceleration factor does not significantly affect the overall results, as no substantial differences were observed in total deformation and internal stress values.

The maximum and average values for the aluminum alloy are presented in Table 5, while the corresponding results for structural steel are given in Table 6.

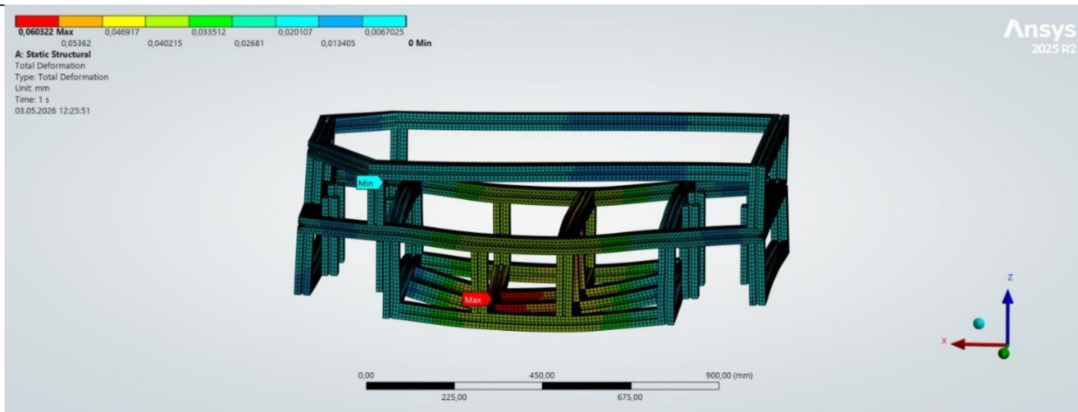

Fig. 9. Total deformation of Aluminium alloy frame without thermal conditions

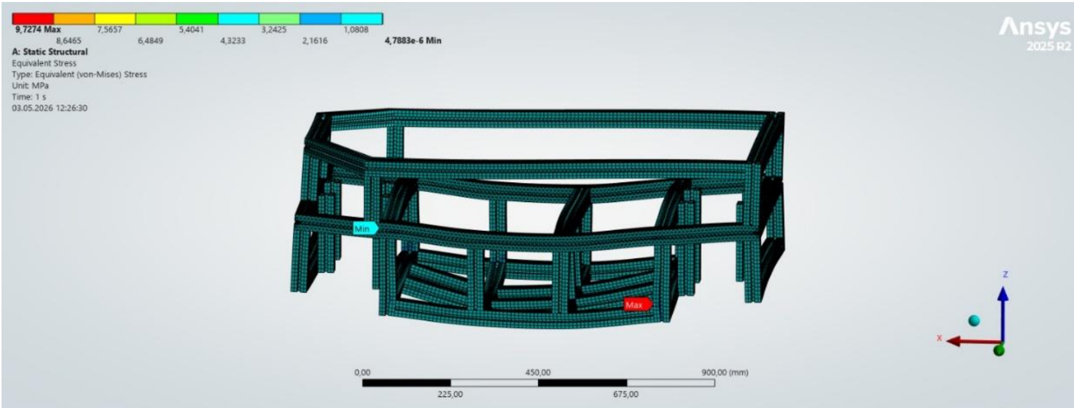

Fig. 10. Equivalent Stress acting of Aluminium alloy frame without thermal conditions

Fig. 11. Equivalent elastic strain experienced by Aluminium alloy chassis without thermal conditions

Table 5. Aluminium Alloy with application of acceleration condition

	Maximum Value	Average Value
Total Deformation (mm)	0,060322	0,017328
Equivalent Stress (MPa)	9,7274	0,26109
Equivalent Elastic Strain	0,000137	0,0000041613

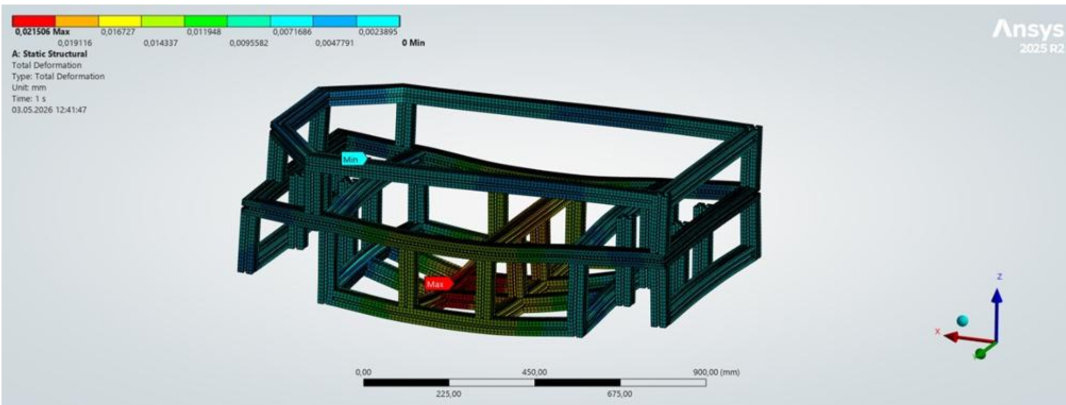

Fig. 12. Total deformation of Structural Steel frame without thermal conditions

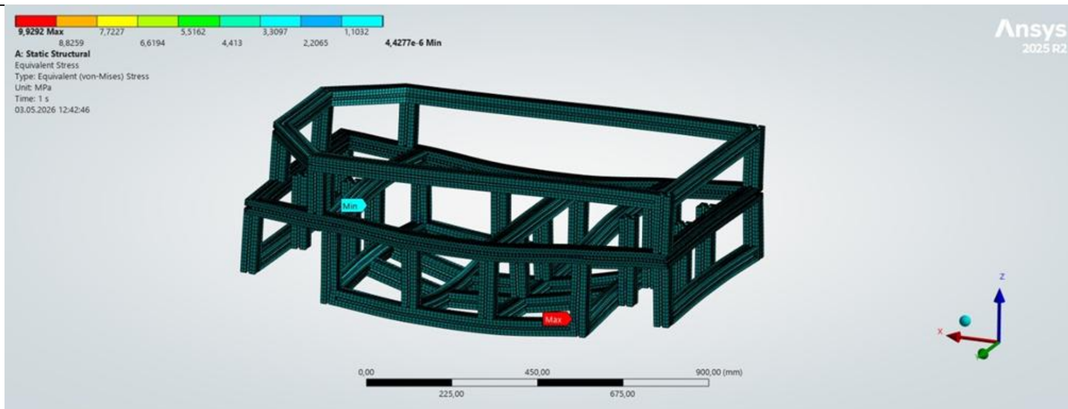

Fig. 13. Equivalent stress of Steel frame without thermal conditions

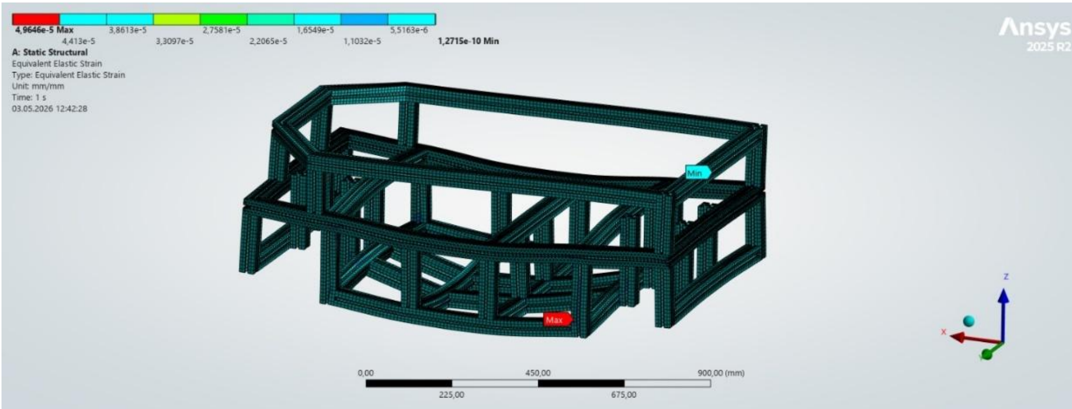

Fig. 14. Equivalent elastic strain of Steel frame without thermal conditions

Table 6. Structural Steel with application of acceleration

	Maximum Value	Average Value
Total Deformation (mm)	0,021506	0,0061624
Equivalent Stress (MPa)	9,9292	0,26032
Equivalent Elastic Strain	0,000049646	0,000001486

3.3 Behavior of frame under load, acceleration, and 35°C temperature condition

The results of the structural analysis performed on the developed robot frame under combined external loading, acceleration effects, and a temperature of 35°C revealed notable differences depending on the mechanical and thermal properties of the selected materials. According to the obtained results, the aluminum alloy frame exhibited higher total deformation compared to the structural steel frame. This behavior is attributed to the lower strength limit and higher coefficient of thermal expansion of aluminum alloy (Figures 14 and 18).

The maximum deformation was observed in the upper rear region of the frame. This is due to the fact that, under the combined influence of external load, acceleration, and elevated temperature, deformation is more pronounced in regions located farther from support points and having lower structural rigidity, whereas minimal deformation occurs in areas near supports and reinforced structural zones. Although the results confirm the overall mechanical stability of the structure, they also indicate the necessity of additional reinforcement in specific regions.

Although equivalent stress values in the aluminum alloy are lower than those in structural steel, equivalent elastic strain values are higher in the aluminum configuration. This is mainly due to the higher stiffness of structural steel, which results in lower deformation under identical loading conditions (Figures 15 and 19).

Thermal deformation analysis further shows that aluminum alloy is more sensitive to temperature-induced changes. This is explained by its higher isotropic linear thermal expansion coefficient compared to structural steel (Figures 17 and 21).

The maximum and average values of total strain, equivalent stress, elastic strain, and thermal deformation for the aluminum alloy are presented in Table 7, while the corresponding results for structural steel are given in Table 8. The obtained results indicate that under elevated temperature operating conditions, the structural steel frame demonstrates better performance in terms of mechanical stability and thermal resistance.

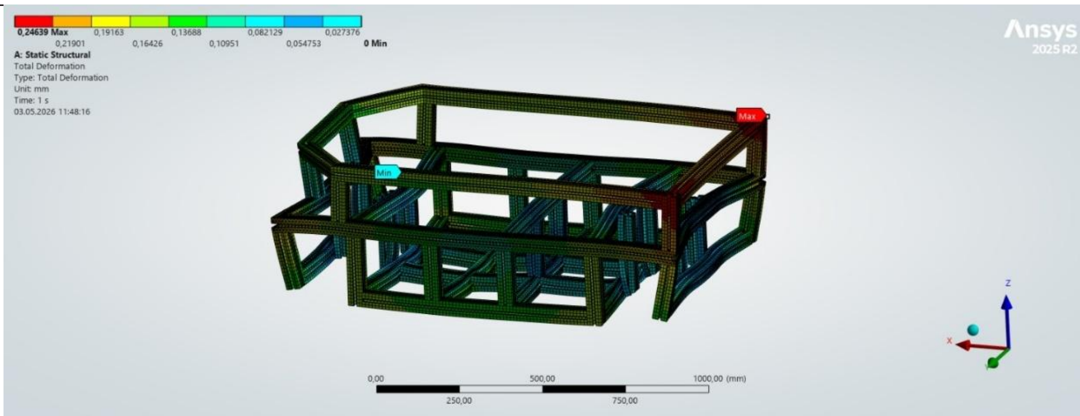

Fig.15. Total Deformation of aluminium alloy frame

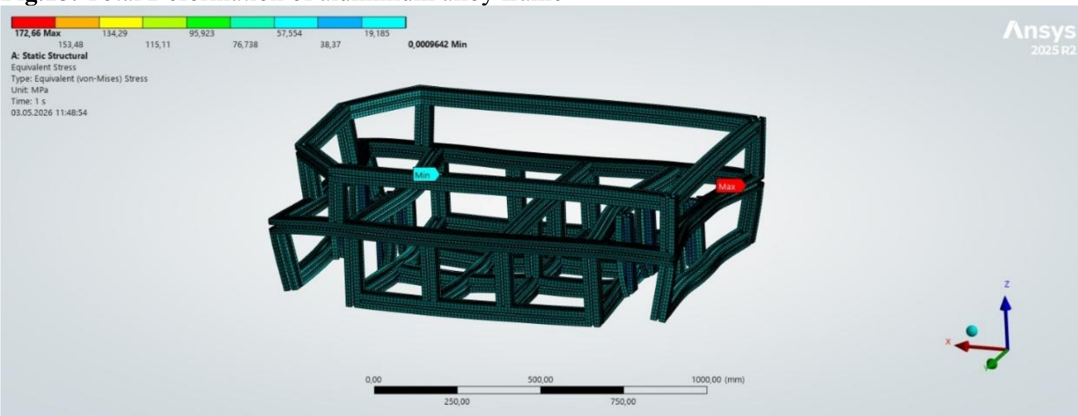

Fig.16. Equivalent stresses of aluminium alloy frame

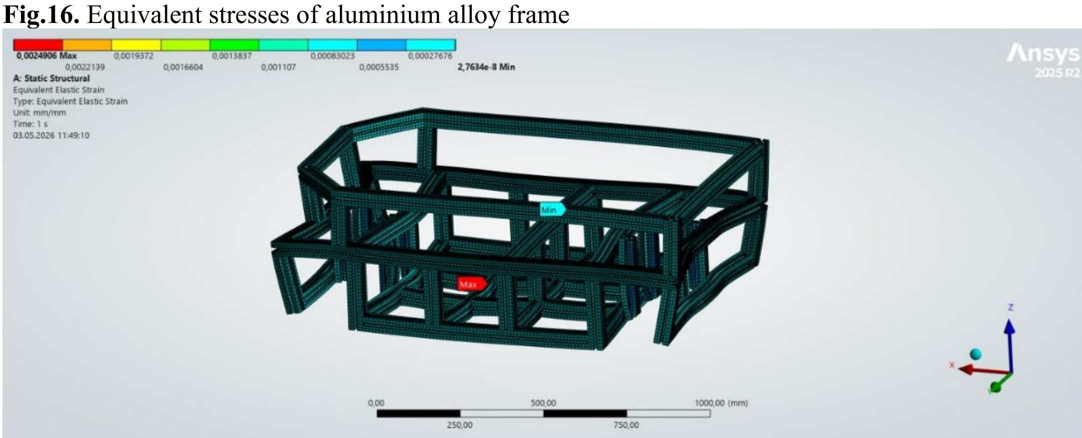

Fig. 17. Equivalent elastic strain of aluminium alloy frame

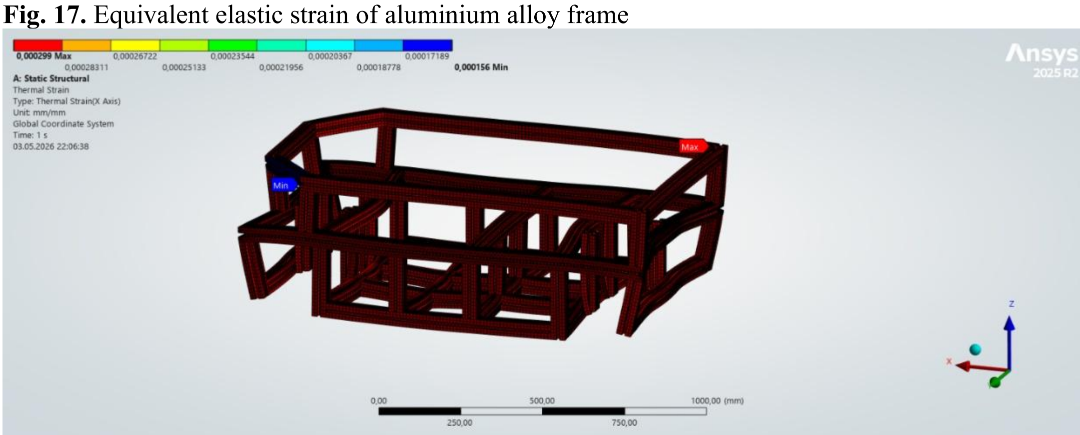

Fig. 18. Thermal strain of aluminium alloy frame

Table 7. Aluminium Alloy with application of thermal and acceleration condition

	Maximum Value	Average Value
Total Deformation (mm)	0,24639	0,10538
Equivalent Stress (MPa)	172,66	4,1806
Equivalent Elastic Strain	0,0024906	0,00007189
Thermal Strain	0,000299	0,00029742

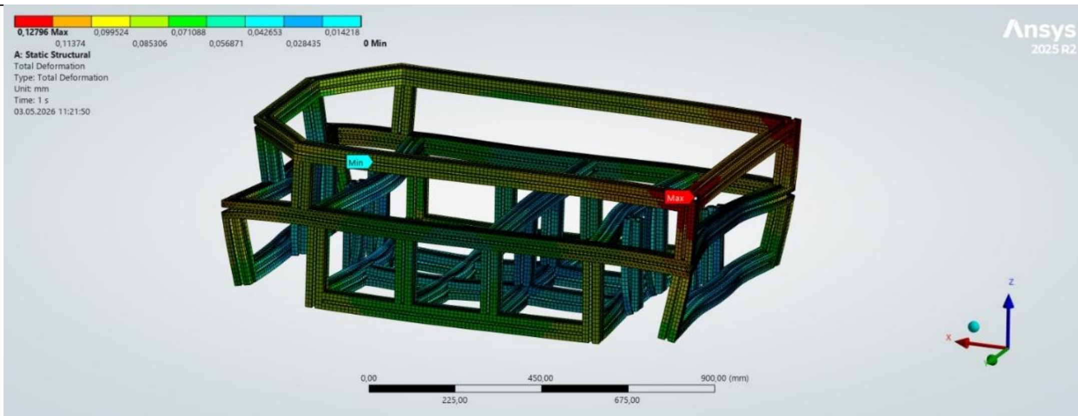

Fig. 19. Total deformation of structural steel frame

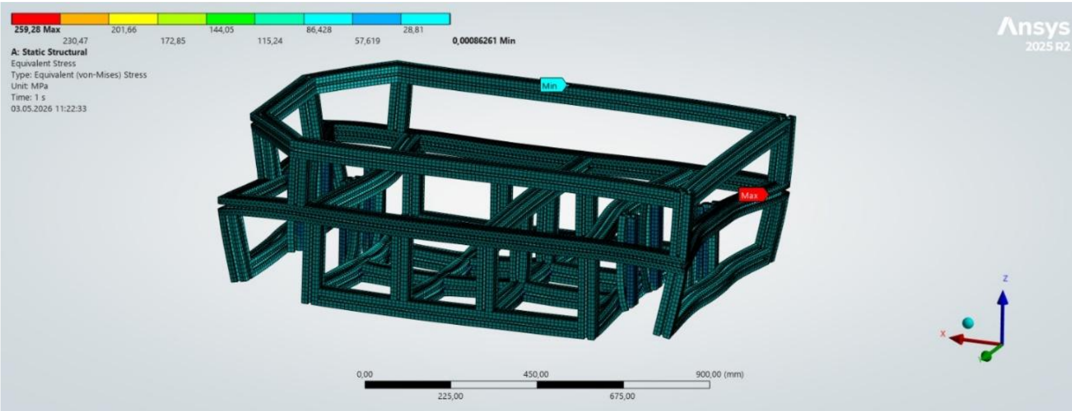

Fig. 20. Equivalent stresses of the structural steel frame

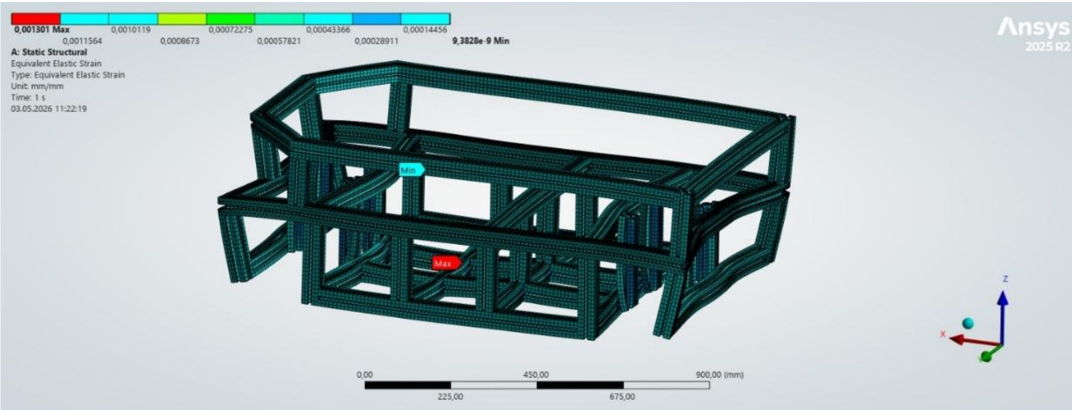

Fig. 21. Equivalent elastic strain of the structural steel frame

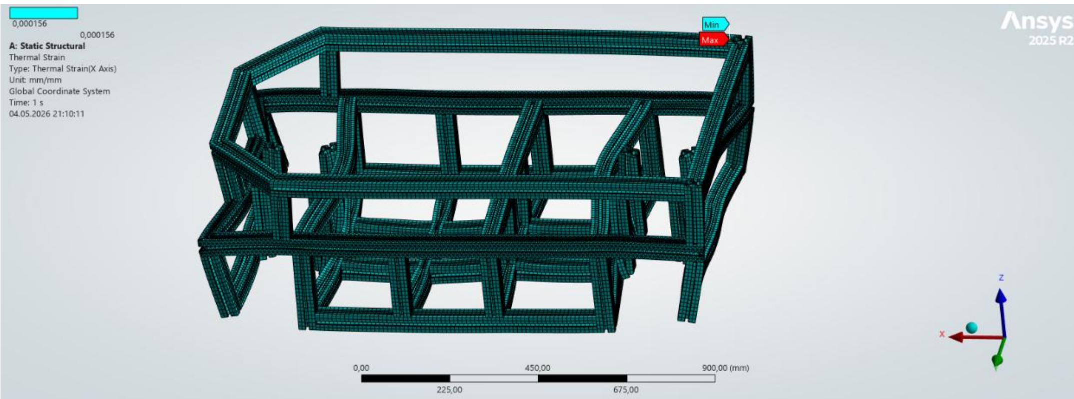

Fig. 22. Thermal strain of the structural steel frame

Table 8. Structural Steel with application of thermal and acceleration condition

	Maximum Value	Average Value
Total Deformation (mm)	0,12796	0,05457
Equivalent Stress (MPa)	259,28	6,0858
Equivalent Elastic Strain	0,001301	0,0000374
Thermal Strain		

Conclusions

The results of the static structural analysis conducted on the developed agricultural robot frame revealed significant differences in the mechanical performance of structural steel and aluminum alloy materials. Throughout all analyzed scenarios, the aluminum alloy structure exhibited greater total deformation compared to structural steel. Under static loading conditions alone, the total deformation of the aluminum model was 2.80 times higher than that of the steel structure. When thermal effects were included, deformation increased further, with the total deformation of the aluminum alloy frame at 35°C being 1.93 times greater than that of structural steel. The acceleration factor had no significant influence on deformation behavior.

In terms of equivalent stress, both materials demonstrated nearly similar values under non-thermal loading conditions. However, under elevated temperature conditions, the equivalent stress in structural steel was approximately 1.50 times higher than in aluminum alloy. This is attributed to the greater stiffness and internal stress absorption capacity of steel.

Equivalent elastic strain results also confirmed that aluminum alloy is more susceptible to deformation. Under standard loading conditions, the elastic strain of the aluminum model was 2.76 times greater than that of structural steel, while under thermal conditions this ratio remained at approximately 1.91.

Although thermal deformation distribution was relatively uniform for both materials, the total thermal deformation of aluminum alloy was greater due to its higher coefficient of thermal expansion. Overall, the analysis indicates that structural steel is a more reliable material for agricultural robot frame construction under high-temperature and complex loading conditions, as it provides lower total deformation, reduced elastic strain, and greater thermal stability.

At the same time, despite its higher deformation tendency under standard operational conditions, aluminum alloy remains a practically viable alternative due to its lighter weight, economic efficiency, and acceptable mechanical performance. Therefore, material selection should be determined based on the robot's operational environment, expected load conditions, and economic considerations.

The findings of this study show strong similarity to the structural analyses performed on three-wheeled robot chassis systems by Avadhoot Rajurkar, Kunal Dangra, Aryan Deshpande, Madhav Gosavi, Tejas Phadtare, and Gajanan Gambhire [11]. In particular, the comparative behavior of aluminum alloy and structural steel in terms of load response, deformation, and stress distribution is consistent with previously reported trends. However, certain differences were identified, primarily resulting not from material properties but from variations in chassis design, geometric configuration, and the number and placement of support points. Specifically, load distribution patterns and deformation zones in the four-wheeled frame differed from those of the three-wheeled model, indicating that structural configuration plays a critical role in overall mechanical performance.

Thus, the results of this research support the principal conclusions of previous scientific studies while also confirming that, alongside material selection, structural optimization is a key factor in effective agricultural robot frame design.

References

[1] Natheer Almtireen, Mutaz Ryalat Robotics in Precision Agriculture: Task-, Platform-, and Evaluation-Oriented Review. Robotics 2026, 15(4), 81; pp. 1-37. https://doi.org/10.3390/robotics15040081

[2] van Dijk, M.; Morley, T.; Rau, M.L.; Saghai, Y. (2021). A meta-analysis of projected global food demand and population at risk of hunger for the period 2010–2050. Nature Food, 2(7), 494–501. https://doi.org/10.1038/s43016-021-00322-9

[3] Falcon, W.P.; Naylor, R.L.; Shankar, N.D. (2022). Rethinking global food demand for 2050. Population and Development Review, 48, 921–957. https://doi.org/10.1111/padr.12479

[4] Ganiboyeva E., Norov B. Kh., Suyunov S., Khudaev I. (2022). Effective use of motor oil resources of the tractor of the company "CLAAS" in the conditions of Uzbekistan. IOP Conference Series: Earth and Environmental Science, 1076(1), 012084. https://doi.org/10.1088/1755-1315/1076/1/012084

[5] Lu, L., Liu, B., Mao, E., Song, Z., Chen, J., & Chen, Y. (2023). Design and optimization of high ground clearance self-propelled sprayer chassis frame. Agriculture, 13(2), 233. https://doi.org/10.3390/agriculture13020233

[6] Reiser, D.; Nannen, V.; Hubel, G.; Griepentrog, H.W. (2019). Design, modelling and control of a novel agricultural robot with interlock drive system. 2019 IEEE/RSJ International Conference on Intelligent Robots and Systems (IROS), 5520–5525. https://doi.org/10.1109/IROS40897.2019.8968449

[7] Abhishek; Khare, G.K. (2025). Design optimization of truck chassis using finite element analysis. International Journal for Research in Applied Science & Engineering Technology (IJRASET), 13(7), 441–452. https://doi.org/10.22214/ijraset.2025.73031

[8] Kuruvilla, J. K., Seth, A., Duttagupta, J., Sharma, S., & Jaiswal, A. (2024). Structural design and analysis of 6-DOF cylindrical robotic manipulators for automated agriculture. In Precision Agriculture for Sustainability (pp. 147–168). Apple Academic Press. https://doi.org/10.1201/9781003435228-10

[9] Irsel, G. (2023). Design of a precision planter chassis using computer-aided engineering and experimental validation. Proceedings of the Institution of Mechanical Engineers, Part C: Journal of Mechanical Engineering Science, 237(22). https://doi.org/10.1177/09544062231159008

[10] Chen, K.; Yuan, Y.; Zhao, B.; Jin, X.; Lin, Y.; Zheng, Y. (2022). Finite element modal analysis and experiment of rice transplanter chassis. International Journal of Agricultural and Biological Engineering,

15(5), 91–100. https://doi.org/10.25165/j.ijabe.20221505.6230
[11] Rajurkar, A., Dangra, K., Deshpande, A., Gosavi, M., Phadtare, T., & Gambhire, G. (2023). Comparative finite element analysis of a novel robot chassis using structural steel and aluminium alloy materials. Engineering Innovations, 7, 61–73. https://doi.org/10.4028/p-45j91B
[12] Ruoyuan Liu, Mingjie Dong, Qi Xiao, Changqi Lv, Ziqiang Zhanglar Design, Analysis, and Experiment of an Automatic Lettuce-Harvesting Mechanism. Chinese Journal of Mechanical Engineering (2025) 38:175 https://doi.org/10.1186/s10033-025-01288-6
[13] Ding, R., Qi, X., Meng, X., Chen, X., Zhang, L., Mei, Y., Li, A., & Ye, Q. (2025). A review on the chassis configurations and key technologies of agricultural robots. Agriculture, 15(22), 2379. https://doi.org/10.3390/agriculture15222379